Averaged model for probabilistic coalescence avalanches in two-dimensional emulsions: Insights into uncertainty propagation

Danny Raj M. and R. Rengaswamy*
150, Mechanical sciences block, IIT Madras, Chennai-600036 India
(Received 16 November 2016; published 23 March 2017)

A two-dimensional concentrated emulsion exhibits spontaneous rapid destabilization through an avalanche of coalescence events which propagate through the assembly stochastically. We propose a deterministic model to explain the average dynamics of the avalanching process. The dynamics of the avalanche phenomenon is studied as a function of a composite parameter, the decay time ratio, which characterizes the ratio of the propensity of coalescence to cease propagation to that of propagation. When this ratio is small, the avalanche grows autocatalytically to destabilize the emulsion. Using a scaling analysis, we unravel the relation between a local characteristic of the system and a global system wide effect. The anisotropic nature of local coalescence results in a system size dependent transition from nonautocatalytic to autocatalytic behavior. By incorporating uncertainty into the parameters in the model, several possible realizations of the coalescence avalanche are generated. The results are compared with the Monte Carlo simulations to derive insights into how the uncertainty propagates in the system.

DOI: 10.1103/PhysRevE.95.032608

I. INTRODUCTION

Immiscible fluids flow as drop and continuous phases when forced through a microchannel. These drops can self-organize to form ordered arrangements as they flow in the channel [1,2]. Bremond and co-workers fashioned a two-dimensional (2D) channel with provisions to drain the excess continuous phase in the system in order to pack drops tightly. In such concentrated emulsion systems, a single coalescence event in any part of the channel can trigger an avalanche of similar events that leads to spontaneous destabilization of the entire assembly [2]. Coalescence avalanches in a 2D concentrated emulsion is a complex phenomenon, which is a result of the many body interactions as the drops flow in the microchannel [3]. Two closely spaced drops (A and B) when pulled apart, create a low pressure in the region between the drops that pulls the interfaces together initiating coalescence [4–6]. Now in a concentrated emulsion when A and B coalesce they are pulled away from other drops in their neighborhood. These neighboring drops experience a force that pulls their interface towards A and B. In Fig. 1(a), drops (A and B) are shown in black; other drops surrounding this pair make an angle θ with them. The magnitude of the force depends on the relative position of the drop (θ) with respect to A and B. The anisotropic nature of coalescence results in a cluster that propagates like fingers in the 2D channel, giving rise to interfaces with high curvature that dynamically relax as the cluster grows. This results in reorganization of the drops in the channel which continuously alters the film thickness and the proximity of the drops to active growing regions of the propagating cluster making the process appear stochastic to an observer.

Recently, we proposed a stochastic model that captures the salient features of this multibody phenomenon [3]. Coalescence is triggered in an assembly of drops on a lattice, and the destabilization front is allowed to propagate stochastically according to a probability rule—experimentally measured by Bremond and co-workers [2]. The probability measure P used in the model quantifies the propensity for coalescence locally in a compact assembly. This measure $P(\theta)$ is a function of orientation of drops θ, which captures the anisotropic nature of propagation. Figure 1(c) shows a snapshot of the experimental results of Bremond and co-workers [2] where one can find avalanches of different sizes. The stochastic model captures the dynamics of the propagation of both small and large avalanches [as shown in Figs. 1(a)–1(g)]. By performing a Monte Carlo study [1], which involves over 10^5 independent realizations of the coalescence propagation, we quantify the average behavior of the system and derive insights into the autocatalytic nature of the avalanching process. The collective stability of the emulsion system is studied as a function of the system properties—which is captured by modifying $P(\theta)$ as $\alpha P(\theta)$—and the size and aspect ratio of the assembly, where α is a number greater than zero that is used to scale the probability function $P(\theta)$.

The stochastic model is a bottom-up approach that views any observation of the complex coalescence problem as a consequence of the interactions at the drop level. For example, the model predicts that the critical $\alpha = \alpha_{cr}$, above which the propagation becomes autocatalytic, depends on the size of the system $\alpha_{cr} = f(N)$ and in the transition region, the time and ensemble-averaged effective number of neighbors is always 3. These observations appear as emergent characteristics of the complex system, and the reason behind why the system exhibits such characteristics is difficult to fathom from the stochastic model. In this article, we propose an alternate route, a top-down approach, to understand the complex nature of coalescence avalanches to answer some of these questions. The simplest deterministic model that directly predicts the averaged behavior of the system is introduced. From a computational view point this would be a more efficient strategy when compared to the stochastic approach which needs a large ensemble of realizations over which averaging and grouping procedures are performed to predict the average system behavior.

Figure 2 presents an overview of how the modeling approaches, although different, can be used in conjunction to uncover the underlying physics of the process. Every time the stochastic model is run, a possible realization of the process is simulated. On the other hand, the averaged model, which

*raghur@iitm.ac.in

 ©2017 American Physical Society

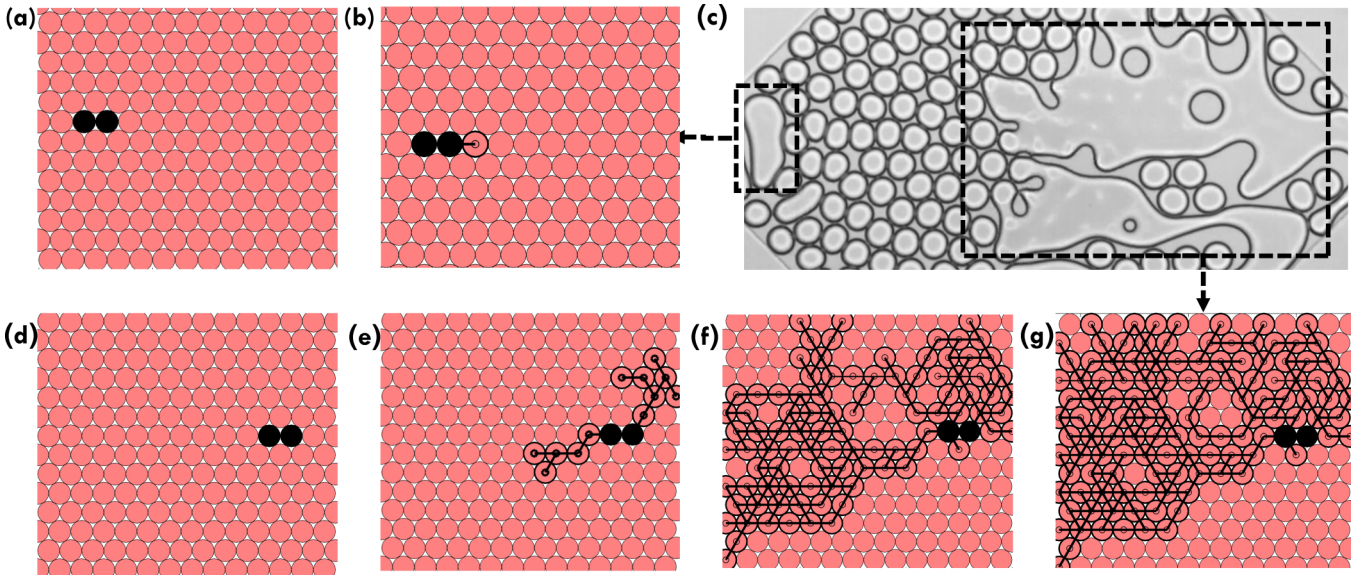

FIG. 1. Coalescence avalanches in a 2D emulsion, experiments [2], and simulation [3]: (a) and (d) trigger events where a pair of drops is allowed to coalesce. (b) Avalanching process stops with just one more coalescence event which results in a small sized avalanche. (c) Experiments of Bremond and co-workers [2] where coalescence avalanches both small and large in size are observed [courtesy: N. Bremond (ESPCI, France)]; (d)–(g) dynamic growth of a large sized avalanche [time (in generations): 1, 5, 15, and 25].

estimates the average ensemble behavior, is a deterministic model that yields the same result for fixed initial conditions and parameter values. However, with the addition of an uncertainty into the various elements of the averaged model, say the initial conditions or the parameters, it may be possible to generate an ensemble of possible realizations. Various interesting questions will arise at this point: By adding a certain uncertainty will it be possible to reconstruct the results of the stochastic model? What uncertainty should be added to the system? How is the uncertainty related to the complex drop movement which is responsible for the stochastic behavior in the first place? In this article, we answer such questions. An equivalence is established between the stochastic and the deterministic models, and a hybrid formulation is proposed to study destabilization of the drop ensembles.

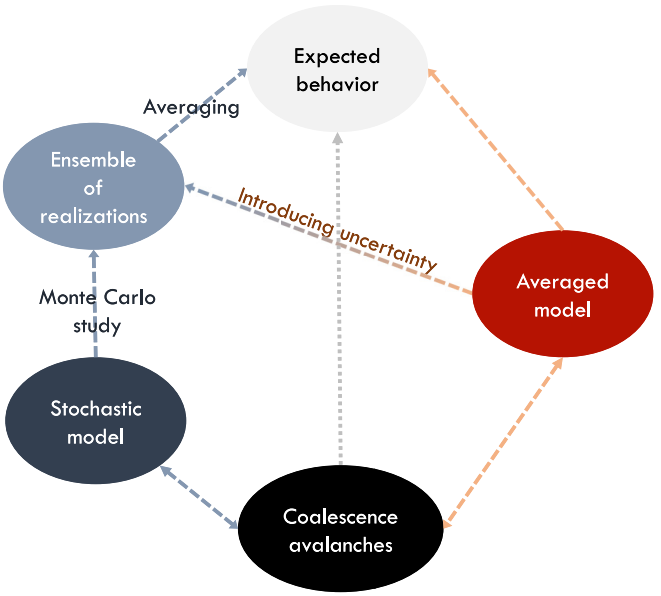

FIG. 2. Modeling schemes to understand the collective averaged behavior of coalescence avalanches in 2D emulsions. There are two ways to model—a stochastic approach and an averaged model (deterministic) approach.

II. AVERAGED MODEL

Once a coalescence event is triggered, it continues to propagate from the active sites that are formed in the growing cluster. An active site is that part of the cluster where there was a recent coalescence event which has created a local low pressure zone that pulls interfaces of neighboring drops to the cluster. Hence, the rate of propagation at any instant in time depends on the number of active sites available for coalescence and the availability of free drops in the neighborhood of these active drops. If β refers to the average number of neighboring drops available per active site, then for X active sites, the rate should be proportional to the term βX. Note that this term also refers to the total number of neighbors available at a given instant in time. Consider two cases (1 and 2) where the number of active sites in case 1 is greater than that in case 2($X_1 > X_2$), but the total number of neighbors available for coalescence is the same $\beta_1 X_1 = \beta_2 X_2$ as shown in Figs. 3(a) and 3(b). The propensity for neighboring drops to coalesce with the cluster depends on the angle these drops make with the active sites due to the anisotropic nature of propagation as shown in Fig. 3(c).

When the angles made by drops with the active sites are lower, the coalescence propagation rate is higher. When the numbers of active sites are greater for a given set of neighboring drops one would expect this angle, on average, to be lower as illustrated in Fig. 3(b). The configuration in (a) contains two active sites and ten associated neighboring drops, and the configuration in (b) has four active drops with

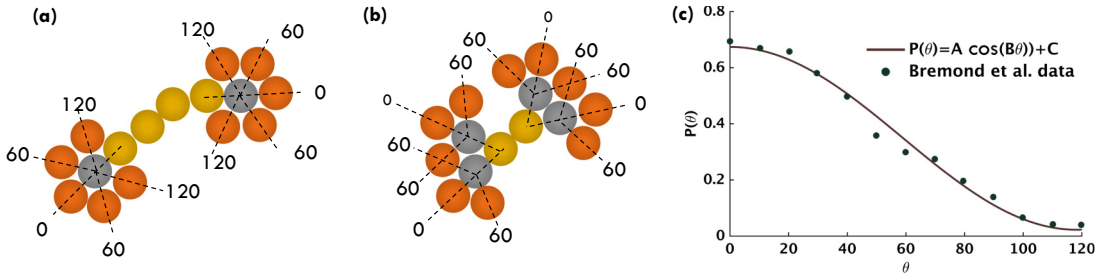

FIG. 3. (a) A configuration of drops that contains two active sites with ten neighbors in total. The angles made by the neighbor drops are marked in the figure. (b) A configuration with ten neighbor drops and four active sites with angles marked in the figure. (c) The probability of propagation as measured by Bremond *et al.* in their experiments [2], which shows the anisotropic nature of propagation. [Note: the average angle made by the configuration in (b) is greater than that in (a). Hence the propagation rate is expected to be greater for (b)].

the same number of neighbors. Comparing the different angles made by the neighboring drops in the two configurations we observe that case (b), which has more active drops, has lower angles than case (a) with less numbers of active drops. The propagation rate due to this effect is captured by the term X^{γ} where the value of γ is a small positive number. If the propagation were to be isotropic, $P(\theta)$ will be a constant, and correspondingly γ will take a value of zero. Hence, the rate of growth of an avalanche (dA/dt) can be represented by the term $k_1\beta X^{1+\gamma}$ as shown in Eq. (1). Here the size of an avalanche A always refers to the numbers of coalescence events that have occurred after the avalanche is triggered

$$\frac{dA}{dt} = k_1\beta X^{1+\gamma}. \tag{1}$$

When there are no active sites or no available neighbors for propagation, the growth term takes a value of zero. For all other situations, it is greater than zero, which captures the unidirectional growth of an avalanche. As drops coalesce to the cluster, they form new active sites. So, the number of coalescence events at a certain time would correspond to the number of active sites formed. Hence the avalanche propagation rate [right-hand side (rhs) of Eq. (1)] will be the same as the rate of the formation of active sites [the first term on the rhs of Eq. (2)]. All the active sites that are produced at a particular instant in time need not result in propagation. Hence one would expect a certain number of active sites to become inactive, and this number would depend on the probability associated with coalescence propagation (the propensity) and total number of active sites at a given instant in time. This reduction in the number of active sites is given by the second term in Eq. (2),

$$\frac{dX}{dt} = k_1\beta X^{1+\gamma} - k_d X. \tag{2}$$

The number of neighbors available per unit active site β for propagation would depend on the size of the avalanche and the way in which the cluster is propagating. This makes it hard to estimate the instantaneous value of β. But on average, we know that when avalanche size is small, the number of neighbors available per active site is maximum, say λ, and it takes a value of zero when the avalanche size is close to the maximum possible size N. Hence the simplest model for β that can be postulated would be a linear model as shown in Eq. (3). The parameter λ represents the maximum neighbors available for coalescence. In a hexagonally close packed arrangement a drop typically has six neighbors, but because neighbors have different tendencies to coalesce this parameter λ will take a value less than 6. Changing the properties, such as viscosity and surface tension, would also change the value of λ. For the case where the surfactant concentration is very high, Gunes and co-workers showed that drops are stable to coalescence by decompression [6]. It is only intuitive to expect the value of λ to be low for such cases. Baret and co-workers showed that by manipulating the surface coverage of the drop phase by the surfactant molecules one can transition from a stable to an unstable configuration [7]. Hence one can also expect the avalanche dynamics to transition to the unstable regime with the manipulation of the parameter λ. One can compute β from the Monte Carlo simulations by counting the effective neighbors and the active sites available at the end of every generation. Monte Carlo simulations are carried out on the stochastic model proposed earlier (an algorithm can be found in Ref. [3]) where propagation is studied on a lattice. A random pair of drops is allowed to coalesce, and propagation is studied as a function of the probability of local coalescence $[\alpha P(\theta)]$. Figure 4 shows how the neighbors available per active site β, computed from the Monte Carlo simulations (scatter plot), vary with the avalanche

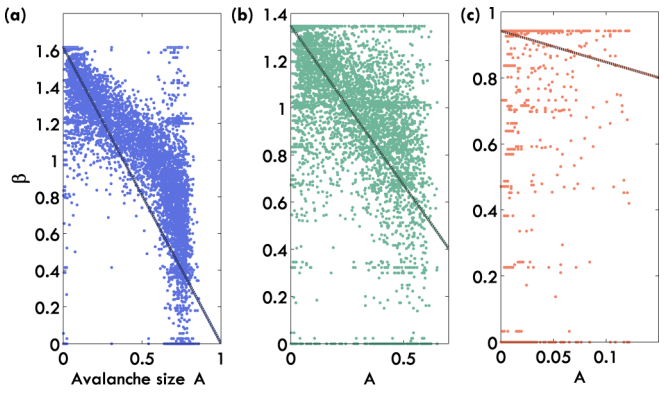

FIG. 4. The number of neighbors per active drop β, plotted as a function of avalanche size from the Monte Carlo simulations (points) and the averaged model [Eq. (3), solid lines] for different values of α (tunable parameter that accounts for the propensity to propagate). (a) $\alpha = 1.2$ higher propensity for coalescence. (b) $\alpha = 1$ (corresponds to the propensity for coalescence as observed by Bremond *et al.* [2] in their experiments). (c) $\alpha = 0.7$ (lower propensity for coalescence).

size (several realizations plotted together) for different values of α. The solid line in Fig. 4 corresponds to the linear model as explained in Eq. (3). One can observe that the linear model approximately captures the relationship between β and A,

$$\beta = -\frac{\lambda}{N}A + \lambda. \tag{3}$$

Since we are solving an initial value problem we need the initial avalanche size a_0 and active site size x_0. For the cases where a single pair of drops triggers an avalanche, a_0 is 1 and x_0 is 2,

$$A(0) = a_0, \qquad X(0) = x_0. \tag{4}$$

We nondimensionalized the equations in an attempt to obtain the minimal set of parameters that governs the dynamics of the system [8]. Expressing all the dependent and independent variables in terms of scaled variables we have Eqs. (7) and (8). The natural choice for the scale of avalanche size which will make the variable $o(1)$ is N, which is the maximum possible avalanche size. Note that N does not refer to the number of drops in the system but the total number of coalescence events possible, which scales as the number of drops n [2]. For example, when $n \times n$ drops are arranged in a hexagonally close packed configuration, the total number of coalescence events possible can be found to be approximately equal to $3n^2 - 4n + 1$,

$$X = X_s\bar{X}, \qquad A = A_s\bar{A}, \qquad t = t_s\bar{t}, \tag{5}$$

$$A_s = N \tag{6}$$

$$\frac{d\bar{X}}{d\bar{t}} = [k_1 t_s \lambda (X_s)^{\gamma}][-\bar{A} + 1](\bar{X})^{1+\gamma} - k_d t_s \bar{X}, \tag{7}$$

$$\frac{d\bar{A}}{d\bar{t}} = \left[\frac{k_1 t_s \lambda (X_s)^{1+\gamma}}{N}\right][-\bar{A} + 1](\bar{X})^{1+\gamma} \tag{8}$$

$$A_s\bar{A}(0) = a_0, \qquad X_s\bar{X}(0) = x_0. \tag{9}$$

One can choose the scales for X_s and t_s based on the growth or the decay dynamics of active sites. The scales for active sites X_s and time t_s as shown in Eq. (10) are chosen based on the growth rates of active sites and avalanche size [from (7) and (8)]. This is an appropriate choice for cases where the dynamics is dominated by the growth of active sites. By grouping the terms in Eq. (7), a new composite parameter τ_D can be obtained, which we call the decay time ratio. It is the ratio of the propensity of the active sites to stop propagating to the propensity to propagate. The scaled equations are (11) and (13), which are governed only by the parameters γ and τ_D,

$$X_s = N, \qquad t_s = \frac{1}{k_1 \lambda N^{\gamma}}, \tag{10}$$

$$\frac{d\bar{X}}{d\bar{t}} = [-\bar{A} + 1]\bar{X}^{1+\gamma} - \tau_D \bar{X}, \tag{11}$$

$$\tau_D = \frac{k_d}{k_1 \lambda N^{\gamma}}, \tag{12}$$

$$\frac{d\bar{A}}{d\bar{t}} = [-\bar{A} + 1]\bar{X}^{1+\gamma}, \tag{13}$$

$$\bar{A}(0) = \frac{a_0}{N}, \qquad \bar{X}(0) = \frac{x_0}{N}. \tag{14}$$

When one scales X_s and t_s based on the decay dynamics, they take the form as shown in Eq. (15). Equations (16)–(18) are the new sets of governing equations and initial conditions based on the revised scaling. These are the scales governing the dynamics of the system when the phenomenon is dominated by the decay of active sites. In this regime, there is an additional parameter that comes into play—the trigger ratio, which is the ratio of the number of initial triggered active sites to the maximum avalanche size possible. This parameter does not play a major role in the dynamics because it is bounded between 0 and 1,

$$X_s = x_0, \qquad t_s = \frac{1}{k_d}, \tag{15}$$

$$\frac{d\bar{X}}{d\bar{t}} = \frac{1}{\tau_D}\left(\frac{x_0}{N}\right)^{\gamma}[-\bar{A} + 1]\bar{X}^{1+\gamma} - \bar{X}, \tag{16}$$

$$\frac{d\bar{A}}{d\bar{t}} = \frac{1}{\tau_D}\left(\frac{x_0}{N}\right)^{\gamma+1}[-\bar{A} + 1]\bar{X}^{1+\gamma}, \tag{17}$$

$$\bar{A}(0) = \frac{a_0}{N}, \qquad \bar{X}(0) = 1. \tag{18}$$

III. AVALANCHE DYNAMICS

All the analyses described in this article are based on the scaled equations. Hence for convenience from henceforth the "bar" over the variables will be dropped. From Eq. (13), we infer that an avalanche stops propagating only if there are no active sites ($X = 0$) or when there are no neighbors available ($\beta \to 0$, which happens only when $A \to 1$). From Eqs. (11) and (13), we can find that $X_{\text{eq}} = 0$ is the only possible steady state for X. This is consistent with the physical picture of coalescence propagation—where once the avalanching phenomenon stops, all the active sites cease propagating. On the other hand, the avalanche size A_{eq} can take any value between 0 and 1 based on the initial conditions and the active site generation or depletion dynamics.

To understand how the avalanche size attains a certain steady value, it is important to study the transient dynamics of the avalanching process. There are two parameters in the governing equations τ_D, γ and the initial conditions (trigger events) that determine the time evolution of the avalanching phenomenon. The parameter γ and the initial conditions do not change the dynamics of the process qualitatively. This is because γ only makes the growth term in the dynamics nonlinear, which increases the growth of active sites and hence the avalanche size. And increasing the initial conditions will speed up the avalanching process by increasing the number of triggers. However, the parameter τ_D controls the propagation dynamics strongly.

When this parameter (the decay time ratio) is very small $\tau_D \ll 1$, which corresponds to cases where the propensity to propagate is very high, the number of active sites starts to increase autocatalytically, which results in a steep rise in the avalanche size with time as seen in Fig. 5(a). The sigmoidal nature of the growth of the avalanche is a characteristic feature of the autocatalytic nature of the avalanching phenomenon akin to reaction systems [9]. During this short period one can simply drop the decay term in Eq. (11) to understand the dynamics of the process which are dominated by the growth kinetics.

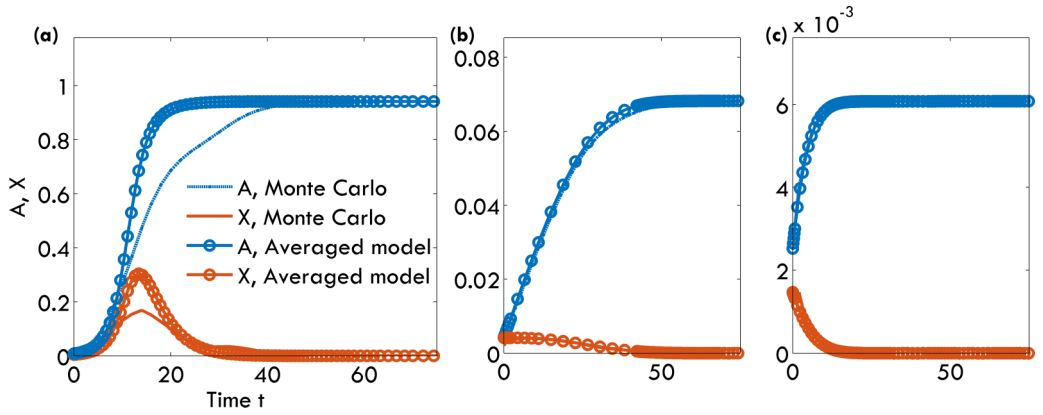

FIG. 5. A comparison of the predictions of Monte Carlo simulations of the stochastic model [3] and the average model for coalescence avalanches. The time evolution of avalanche size and active sites is plotted for different values of the parameters α, τ which quantify the propensity to propagate. The scales used to normalize the avalanche size, active site number, and time are based on the growth kinetics: Eqs. (11) and (13). (a) Averaged model with $\tau_D = 0.28, \gamma = 0.1$ exhibit autocatalytic propagation characterized by the sigmoidal rise in the time evolution of the avalanche size; Monte Carlo simulations are carried out on a 14×14 lattice with $\alpha = 1.9$. (b) Averaged model with $\tau_{D,\mathrm{cr}} = 0.57, \gamma = 0.1$, a critically autocatalytic condition characterized by a maximum in the number of active sites at $T_s = 0$; Monte Carlo simulations: 14×14 lattice with $\alpha = 0.84$. (c) Averaged model with $\tau_D = 0.68, \gamma = 0.1$, and nonautocatalytic propagation characterized by the pseudofirst order response (nonsigmoidal); Monte Carlo simulations: 14×14 lattice with $\alpha = 0.5$.

As the propagation continues the number of neighbors that are available for coalescence decreases. This is because as A goes closer to unity the value of β goes close to zero [from Eq. (3)], which slows down the growth of active sites and the avalanching process as seen in Fig. 5(a) when $T_s > 20$. Hence the number of active sites X starts decreasing and so does the avalanche size growth rate, and A approaches a steady value of A_{eq}. The decay term in Eq. (11) dominates as β becomes very small and eventually takes X to $X_{\mathrm{eq}} = 0$, which is the only possible steady state value for active sites. As the decay time ratio (τ_D) is reduced, the peak value of X decreases, and when τ_D is $\tau_{D,\mathrm{cr}}$, the system reaches a critical state where the maxima in $X(t)$ are found at $T_s = 0$ as shown in Fig. 5(b). This is the point in the parameter space where the behavior of the system switches from autocatalytic to nonautocatalytic. Note that the value of $\tau_{D,\mathrm{cr}}$ varies with the parameter γ.

A further increase in the value of τ_D results in the nonautocatalytic time evolution of avalanche size as shown in Fig. 5(c). The number of active sites reduces with time and goes to its steady value of zero. The positive number of active sites results in the propagation of the avalanche as it slowly increases to a steady value. The time evolution is no longer sigmoidal but exponential. This is because when $A \ll 1$, the value of $\beta \approx \lambda$ [from Eq. (3)] a constant, which makes Eq. (13) a pseudofirst order equation with a weak nonlinearity introduced by the parameter γ. This can be expressed approximately using the functional form $A_{\mathrm{eq}}[1 - e^{-\sigma t} + O(\gamma)]$. Similarly, from Eq. (11) we can observe that as τ_D increases, the first term on the right-hand side becomes insignificant, which makes the active sites decay with a first order dynamics as seen in Fig. 5(c) (the red curve).

Figure 5 also shows a good quantitative match between the results of the averaged model and that of the Monte Carlo simulations of the stochastic model, except for the case of $\alpha = 1.9$ where the deviation from the standard sigmoidal evolution results in a slight mismatch. Monte Carlo simulations of the avalanche size and number of active sites for a system 14×14 (in size) is compared with an averaged model for different propensities for avalanche propagation. From the comparison made in Fig. 5, we observe that the propensity for propagation in the stochastic model (characterized by the parameter α) is inversely proportional to the decay time parameter τ_D. In the stochastic model, time is measured in terms of generations without a specific scale factor. For the averaged model the time is scaled by $t_s = \frac{1}{k_1 \lambda N^\gamma} = \frac{\tau_D}{k_d}$. To compare the results, the time in the stochastic model is scaled by choosing a suitable k_d, and once the decay time parameter τ_D is fixed, we observe that the averaged model predicts the ensemble-averaged transient dynamics quite well.

The neighbors available for propagation are characterized by the parameter β, which is explained in Eq. (3). This parameter contains information on the packing characteristics of the 2D ensemble and the probability to coalesce. A simple linear model for the dependence of this parameter on the avalanche size has been used in our simulations. We observed that the results of the averaged model were robust to minor perturbations in the functional form of β. If one were to change the aspect ratio of the ensemble and study the kinetics, one would expect this parameter β to change appropriately. It would be interesting to understand the connection between the various geometric parameters and the form for β.

IV. THE AVERAGED MODEL VS THE STOCHASTIC MODEL: AN EQUIVALENCE

The averaged model captures the autocatalytic nature of the process. By varying the decay time ratio τ_D, we are able to observe two characteristic regimes as observed in the Monte Carlo simulations: one where the time evolution of the avalanche size is sigmoidal (autocatalytic) and the other where it is not (nonautocatalytic). The parameter τ_D is inversely proportional to the parameter λ [as seen in Eq. (12)], which characterizes the maximum number of effective neighbors available for propagation. In the Monte

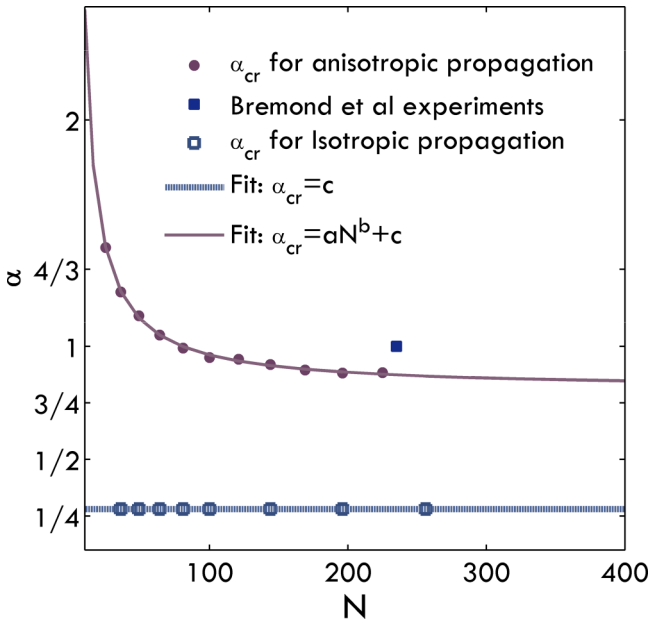

FIG. 6. Plot of α_{cr}vs$N$ that divides the parameter space into two regions: the region above the solid line corresponds to the autocatalytic propagation, whereas that region below it corresponds to the nonautocatalytic propagation regime. The solid line with the circular bullets corresponds to the case where propagation is anisotropic, and the solid line with the square bullets corresponds to the case where the propagation is isotropic. The results of Bremond *et al.* [2] (anisotropic propagation) lie in the autocatalytic region. The solid line for the anisotropic propagation has been approximated as a power law with a constant. However, for the isotropic case α_{cr} is not a function of the N size of the system ($\alpha = \alpha_{cr}$). The probability of propagation at the drop level for the isotropic case is $P(\theta) = \alpha$. When $P(\theta) \approx 0.28$, there is a sharp transition to autocatalytic behavior.

Carlo study, a continuation parameter α was employed to study the effect of probability on propagation, and we observe from Fig. 5 that the parameter τ_D is inversely proportional to α. Hence one can expect λ to be proportional to this parameter α as shown in Eq. (19). This is consistent with the physical picture of coalescence where, when the propensity to coalesce is large, the value of α is large, which corresponds to a large value for the available neighbors λ and a small value of τ_D, respectively. We know that there is a critical value $\tau_{D,\mathrm{cr}}$ which divides the space into autocatalytic and nonautocatalytic parts. Hence one can arrive at a scaling as shown in Eq. (20). This is a scaling that is like the one predicted by the Monte Carlo study as shown in Fig. 6. Hence one can establish equivalence between the two different representations of the same physical process,

$$\tau_D = \frac{k_d}{k_1 \lambda N^{\gamma}} = \frac{k_d}{k_1 (\alpha\varepsilon) N^{\gamma}} = k_r \alpha^{-1} N^{-\gamma}, \tag{19}$$

$$\alpha = \frac{k_r}{\tau_{\mathrm{cr}}} N^{-\gamma}. \tag{20}$$

From Fig. 6, which shows the results of the Monte Carlo simulations, one can observe that the size dependence of α can be adequately represented by the functional form $\alpha = aN^{-1.013} + bN^0$. This would mean that the parameter γ is a function of N. Hence we estimate the exponents from the Monte Carlo data for two asymptotic regions: small N and large N. When the size of system N is small, we observe that γ assumes a value of approximately 0.3 [see Eqs. (21) and (22)],

$$\alpha = aN^{-\gamma},$$
$$a = 3.63, \qquad \gamma = 0.3, \tag{21}$$
$$\frac{k_r}{\tau_{\mathrm{cr}}} = 3.63, \qquad \gamma = 0.3. \tag{22}$$

For large N the curve plateaus, and the parameter γ assumes a value of zero, which makes it independent of size. Equations (23) and (24) show the equivalence for large N,

$$\alpha = aN^{-\gamma},$$
$$a = 0.81, \qquad \gamma = 0, \tag{23}$$
$$\frac{k_r}{\tau_{\mathrm{cr}}} = 0.81, \quad \gamma = 0. \tag{24}$$

The power law dependence of α on N was an emergent characteristic in the stochastic framework. It was not obvious why such a dependence should be observed. But the deterministic averaged model allows us to explain this dependence using physical arguments according to which the parameter γ is a result of the anisotropic nature of propagation. We also observe that the dependence of propagation on this anisotropic nature of propagation reduces with the increase in system size N. According to this hypothesis, if the propagation were to be isotropic (probability is independent of the angle made by the neighbor), then the critical curve in Fig. 6 should become flat.

To confirm the hypothesis, simulations are performed using a local propagation probability $P(\theta) = \alpha$. Here α is a parameter, which is not a function of θ, that quantifies the propensity for isotropic propagation at the drop level. Using this new definition for the probability which characterizes a system exhibiting isotropic propagation, we reconstruct the parameter space plot (α, N), which is shown in Fig. 6. Now when the value of $\alpha > 0.28$, we observe that the system transitions critically from a dominant nonautocatalytic behavior (region below the dotted curve) to an autocatalytic behavior for all system sizes.

V. A HYBRID FORMULATION

The averaged model in Eqs. (11) and (13) can be solved for different values of τ_D. As seen earlier, depending on the value of τ_D, the avalanche size will reach a corresponding equilibrium value of A_{eq}. As the parameter τ_D is varied, A_{eq} changes smoothly as shown in Fig. 7. When the value of τ_D is low, A_{eq} is close to unity, which corresponds to the autocatalytic propagation of coalescence, and with an increase in τ_D, there is a transition from this regime to a nonautocatalytic regime which reduces the value of A_{eq}. Increasing the value of the parameter γ reduces the interval across which this transition occurs as observed from Fig. 7. In the context of the stochastic framework for a given trigger (initial condition) an uncertainty may arise from the choice of τ_D. Hence if we view τ_D as a random variable with a particular probability distribution, it would correspondingly result in distribution for the probability of avalanche sizes.

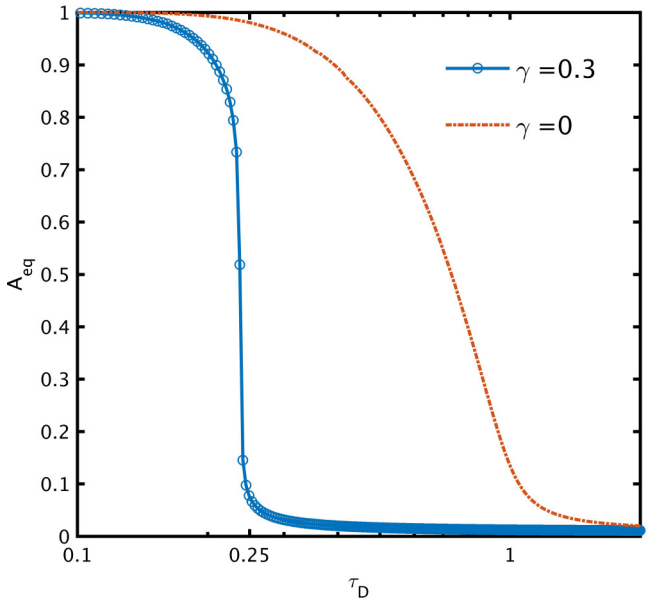

FIG. 7. Equilibrium avalanche size A_{eq} as a function of the decay time ratio τ_D for different values of γ. There is a sharp transition from autocatalytic propagation, which results in large values of A_{eq}, to nonautocatalytic propagation, which results in hardly any propagation (low values of A_{eq}).

From Fig. 5, one can observe that the averaged model can capture all possible features of the kinetics of avalanche growth by simply sampling the parameter τ_D. Hence it is reasonable to use the averaged model to reconstruct the results of the Monte Carlo simulations. The parameter τ_D, which we call the decay time ratio, is a combination of the parameters k_d/k_1—which characterizes the net propensity for coalescence to stop propagating, λ—the neighbors available for propagation as the cluster grows and moves inside the channel, and N^{γ}—the effect of anisotropy in the overall propagation of the cluster. All the above-mentioned parameters change—as the cluster grows, moves, and reorganizes—inside the channel. Hence the time-averaged behavior of every realization of the avalanching phenomenon can be associated with a particular value of τ_D. One may think of other ways to add uncertainty to the process, which includes modifying the number of neighbors available β at an instant of time into $\beta = \beta_0(1 + R)$, where R is a random perturbation or sampling τ_D at every time instant as an avalanche evolves. These methods were not able to capture the entire range of possible avalanche sizes the way uncertainties in τ_D could.

If one were to sample for τ_D from an arbitrary range, say [0.4,1], which is to the right of the transition region, one would expect only avalanches of very small sizes. Another range, say [0.01,0.1] to the left of the transition region, would correspond to large avalanche sizes only. Hence if one wishes to observe both large and small avalanches in the ensemble simulations, it would be necessary to sample near the transition region. The choice for the distribution which should be used for sampling τ_D is not obvious at all. From the nature of the problem, it is very difficult to propose a distribution to sample τ_D rationally. But intuitively, after we select a range of τ_D, one can use a uniform distribution to sample from that range, a suitably scaled lognormal distribution, or a truncated normal distribution with the mean around the transition region.

Algorithm. (1) Choose a probability distribution $P(\tau_D)$ for sampling τ_D. (2) Choose a value of τ_D based on $P(\tau_D)$. (3) Estimate the equilibrium avalanche size using the averaged model [Eqs. (11) and (13)]. (4) Repeat steps 2 and 3 for $\sim 10^5$ times. (5) Calculate the probability of an avalanche as a function of its size.

We choose a lognormal distribution with arbitrary variance and mean for sample τ_D from the transition region as shown in Fig. 8(a). Using the above algorithm, we carry out a Monte Carlo simulation to estimate the probability of the avalanche as a function of its size. From Fig. 8(c) we observe that the avalanche probability shows a characteristic hump as observed in the Monte Carlo simulations of the stochastic framework. This choice of the distribution for sampling τ_D does not affect the qualitative features of the avalanche-probability curve. It is very interesting and nonobvious that a simple averaged description of a multibody phenomenon with uncertainty imposed in the parameters can explain the ensemble-averaged stochastic collective behavior of the same. This exercise shows that it is possible to build a connection between population-kinetics based models (continuum in the number of drops) and stochastic framework (entity level models).

We had shown, through the stochastic framework, that propagation can be completely nonautocatalytic (for low values of α) or completely autocatalytic (for high values of α). This can also be observed using the hybrid formulation by sampling τ_D from different regions on either side of the transition zone as shown in Figs. 8(a), 8(b), and 8(d). However, it is still not clear how the uncertainties in the operating conditions and the complexities that arise due to the multibody interactions result in a probability distribution function for τ_D. Identifying a correlation between physical processes and uncertainties that result from its complexity is an open problem which may be of interest in different fields.

VI. UNCERTAINTY IDENTIFICATION

The probability of an avalanche as a function of its size that one arrives at with the hybrid formulation—as shown in Fig. 8(b)—only qualitatively captures the features of the results of the Monte Carlo simulations [3]. This is because the uncertainty that is introduced in the parameters of the averaged model is arbitrary. By comparing the results of the Monte Carlo simulations [3] with that of the averaged model (A_{eq}vsτ_D), we extract the uncertainty in τ_D that should have been employed in the hybrid model to obtain a quantitative match. Figure 9(a) shows the A_{eq}vsτ_D data that were used to relate the observed equilibrium avalanche size to the parameter in the averaged model, plotted along with the probability distributions for sampling τ_D, extracted from the Monte Carlo simulations for different system sizes.

We observe a characteristic feature for the probability distribution for τ_D when the system size is very small. This corresponds to the case which does not show a hump. As the number of drops in the assembly increases, there is an emergence of an additional feature—a peak near the transition τ_D region—which is similar to the probability distribution for τ_D used in the hybrid model. The uncertainty in the

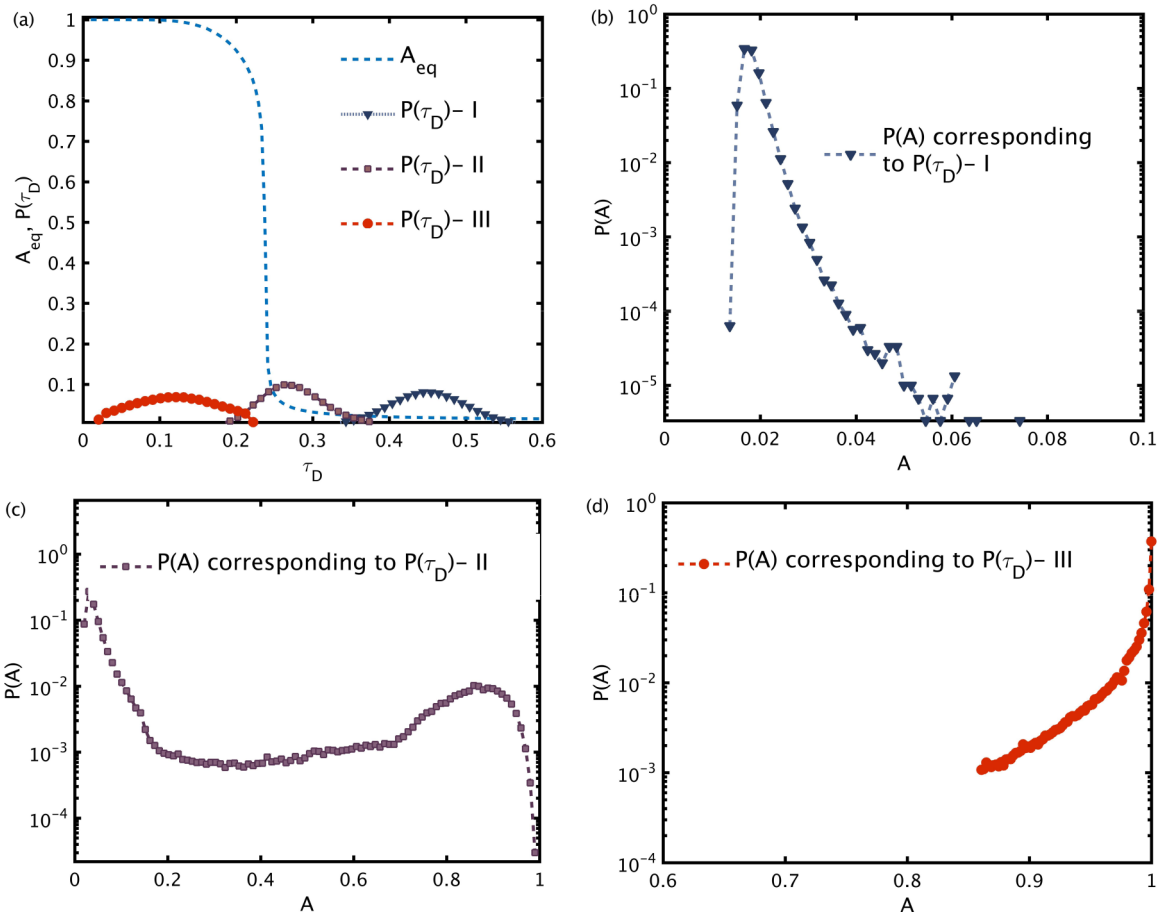

FIG. 8. (a) A plot of A_{eq} as a function of τ_D. The parameter τ_D is sampled in three different regions. $P(\tau_D) - \text{I}$ corresponds to τ_D sampled on the rhs of the critical region, $P(\tau_D) - \text{II}$ corresponds to τ_D sampled in the critical region, and $P(\tau_D) - \text{III}$ corresponds to τ_D sampled on the lhs of the critical region (probability distributions with arbitrary mean, variance, and bounds were used to sample τ_D in the regions of interest). (b) The probability of an avalanche as a function of its size corresponding to the distributions for $P(\tau_D) - \text{I}$, which contains only avalanches of smaller sizes. (c) The probability of an avalanche as a function of its size corresponding to the distributions for $P(\tau_D) - \text{II}$. The probability distribution captures the emergence of a hump as observed in the Monte Carlo simulations [3]. (d) The probability of an avalanche as a function of its size corresponding to the distributions for $P(\tau_D) - \text{III}$, which consists of avalanches of large sizes.

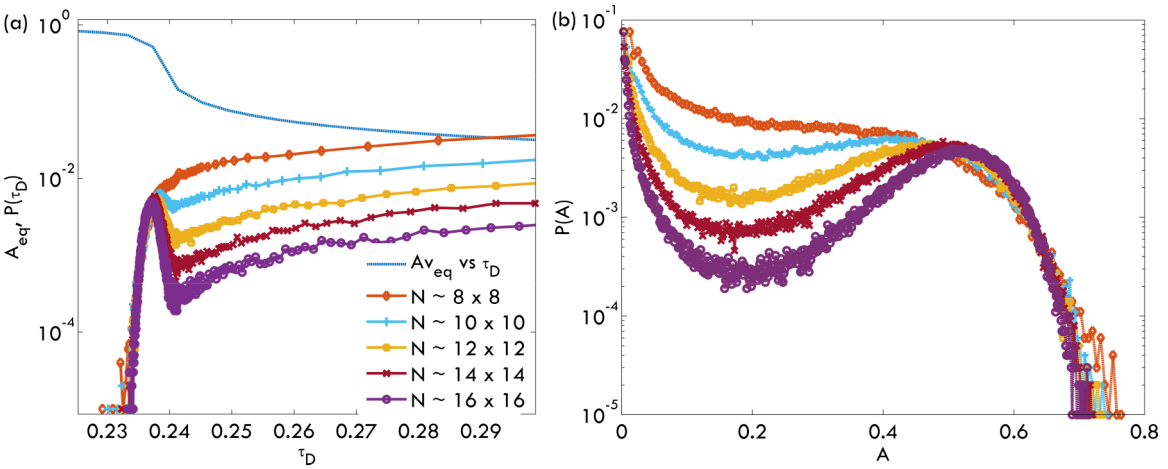

FIG. 9. (a) A plot of A_{eq} vs τ_D from the averaged model under conditions $\gamma = 0.3, A(0) = 0.1, X(0) = 0.1$. The uncertainty that has to be incorporated in the parameter τ_D to explain the results from the Monte Carlo simulations as shown in (b). (b) Monte Carlo simulation under conditions $N = 8^2 - 16^2, \alpha = 1$, aspectratio ≈ 1 (for the algorithm in Ref. [3]). The probability of an avalanche as a function of its size A.

process arises out of the complex motion of the drops and the growing cluster, which change the packing, the film thickness, and the surfactant concentration in the 2D emulsion system, continuously perturbing the avalanching phenomenon making it stochastic. The probability of τ_D that we have extracted is related to this complex behavior. It will be an interesting pursuit to identify how the complex self-organization and the rearranging cluster contribute to the uncertainty in the parameters of the averaged model.

VII. CONCLUSION

A deterministic model is proposed which predicts the averaged behavior of a stochastic avalanching phenomenon in 2D emulsions. Although the system under consideration is a spatially extended complex interacting system, the averaged behavior is explained by a simple dynamical model which considers the time evolution of the population of active sites and available neighbors to explain the kinetics of avalanche growth. Using suitable physical arguments, functional forms for the growth and death of active sites and avalanche growth are proposed. The sets of parameters that govern the dynamics are obtained through an order one scaling analysis which includes the decay time ratio—which is the ratio between the propensity to cease coalescence and propagate and γ, which characterizes the anisotropy in the local propagation as observed by Bremond and co-workers [2] in their experiments. We arrive at a power law scaling that relates the propensity to coalesce to the size of the system through the propagation anisotropy in the droplet system. This explains the size effects observed in the transition of coalescence propagation from nonautocatalytic to autocatalytic behavior. We confirm our hypothesis using Monte Carlo simulations. The averaged model can capture both the autocatalytic and the nonautocatalytic nature of coalescence propagation upon variation of the decay time ratio. A hybrid formulation is proposed which involves introducing stochasticity or uncertainty to the decay time ratio to capture the nonmonotonic avalanche probability as observed in the Monte Carlo simulations; this establishes a direct equivalence between the stochastic and the deterministic descriptions for the avalanche phenomenon.

ACKNOWLEDGMENT

The authors thank N. Bremond (ESPCI, France) for sharing video results not available in the literature. This work was partly funded by the Department of Science and Technology, India for the project on droplet microfluidics.

[1] B. M. Jose and T. Cubaud, Microfluid. Nanofluid. **12**, 687 (2012).
[2] N. Bremond, H. Doméjean, and J. Bibette, Phys. Rev. Lett. **106**, 214502 (2011).
[3] Danny Raj M. and R. Rengaswamy, Soft Matter **12**, 115 (2016).
[4] L. G. Leal, Phys. Fluids **16**, 1833 (2004).
[5] N. Bremond, A. R. Thiam, and J. Bibette, Phys. Rev. Lett. **100**, 024501 (2008).
[6] D. Z. Gunes, X. Clain, O. Breton, G. Mayor, and A. S. Burbidge, J. Colloid Interface Sci. **343**, 79 (2010).
[7] J. C. Baret, F. Kleinschmidt, A. E. Harrak, and A. D. Griffiths, Langmuir **25**, 6088 (2009).
[8] W. B. Krantz, *Scaling Analysis in Modeling Transport and Reaction Processes: A Systematic Approach to Model Building and the Art of Approximation* (Wiley-Blackwell, Hoboken, NJ, 2007).
[9] H. S. Fogler, *Elements of Chemical Reaction Engineering*, The Prentice Hall International Series in the Physical and Chemical Engineering Sciences (Prentice Hall, Upper Saddle River, NJ, 2008).